Cell, Vol. 106, 183–194, July 27, 2001, Copyright ©2001 by Cell Press

Multiple Gln/Asn-Rich Prion Domains Confer Susceptibility to Induction of the Yeast *[PSI$^+$]* Prion

Lev Z. Osherovich[1] and Jonathan S. Weissman
Howard Hughes Medical Institute
Department of Cellular and Molecular Pharmacology
University of California, San Francisco
513 Parnassus Avenue
San Francisco, California 94143

Summary

The yeast prion *[PSI$^+$]* results from self-propagating aggregates of Sup35p. De novo formation of *[PSI$^+$]* requires an additional non-Mendelian trait, thought to result from a prion form of one or more unknown proteins. We find that the Gln/Asn-rich prion domains of two proteins, New1p and Rnq1p, can control susceptibility to *[PSI$^+$]* induction as well as enhance aggregation of a human glutamine expansion disease protein. *[PSI$^+$]* inducibility results from gain-of-function properties of New1p and Rnq1p aggregates rather than from inactivation of the normal proteins. These studies suggest a molecular basis for the epigenetic control of *[PSI$^+$]* inducibility and may reveal a broader role for this phenomenon in the physiology of protein aggregation.

Introduction

Infectious, self-propagating protein aggregates (prions) constitute a conformational mechanism of inheritance. Originally described as mammalian pathogens (Prusiner, 1998), prions have recently been shown to underlie a number of non-Mendelian traits in fungi (Wickner et al., 1999). While the prion proteins responsible for these various phenomena are otherwise unrelated, a common feature of prion conversion is the formation of β-sheet-rich, amyloid aggegrates. In mammals, prions cause neurodegeneration and death, but in *Saccharomyces cerevisiae*, they allow the epigenetic control of protein activity, which can in certain circumstances prove adaptive (Eaglestone et al., 1999; True and Lindquist, 2000).

The best-characterized yeast prions are *[URE3]* and *[PSI$^+$]*, which result from the aggregation of the nitrogen catabolism repressor Ure2p and the translation termination factor Sup35p, respectively. Incorporation of these proteins into prion aggregates diminishes their normal activity, emulating Mendelian loss-of-function mutations; for example, *[PSI$^+$]* causes the suppression of certain nonsense mutations. The prion properties of Ure2p and Sup35p depend on glutamine- and asparagine-rich (Gln/Asn-rich) domains at the amino terminus of each protein (Serio and Lindquist, 1999; Wickner et al., 1999). These prion domains are dispensable for the normal functions of their proteins and are modular, conferring the ability to aggregate when transferred to other proteins (Wickner et al., 2000).

[1] Correspondence: lxoshe@itsa.ucsf.edu

Genomic searches for Gln/Asn-rich domains similar to the Sup35p prion domain have led to the identification of prion domains in two previously uncharacterized proteins, New1p and Rnq1p (Michelitsch and Weissman, 2000; Santoso et al., 2000; Sondheimer and Lindquist, 2000). When the Gln/Asn-rich regions of these proteins were fused to the C-terminal translational termination domain of Sup35p, the resulting fusion proteins could reversibly aggregate to form stably heritable prion states, termed *[NU$^+$]* and *[RPS$^+$]*, which emulated the *[PSI$^+$]* nonsense suppression phenotype. Full-length Rnq1p exists predominantly in an aggregated form in a number of laboratory strains, but this prion state causes no apparent change in phenotype (Sondheimer and Lindquist, 2000).

Glutamine-rich aggregates are also associated with human disease (Perutz, 1999). Several heritable neurodegenerative diseases including Huntington's Disease and a variety of spinocerebellar ataxias are caused by expansion of CAG codons leading to the production of proteins with long polyglutamine (polyGln) tracts. In vivo, these aberrant proteins form inclusions in affected neurons that correlate with neurodegeneration. Furthermore, expanded polyGln tracts within the Huntingon's Disease protein cause it to form self-seeding amyloid fibrils in vitro (Scherzinger et al., 1999). The structural basis of Gln/Asn-rich aggregation is thought to involve formation of "polar zippers" in which the β sheets are stabilized by a network of hydrogen bonds involving glutamine and aspargine sidechains (Perutz et al., 1994).

Although Gln/Asn-rich domains have an inherent propensity to form amyloid aggregates in vitro, cellular factors strongly modulate the formation, propagation, and toxicity of such aggregates in vivo. Notably, the propagation of *[PSI$^+$]* in yeast as well as of polyGln aggregates in yeast, worms, and mammalian cells can be modulated by Hsp104p, a yeast chaperone involved in thermal tolerance and disaggregation of misfolded proteins (Chernoff et al., 1995; Lindquist et al., 1995; Carmichael et al., 2000; Krobitsch and Lindquist, 2000; Satyal et al., 2000). Elevated levels of Hsp70 chaperones can also ameliorate the effect of polyGln protein aggregation and can influence the efficiency of *[PSI$^+$]* propagation in yeast (Chernoff et al., 1999; Warrick et al., 1999; Muchowski et al., 2000).

In addition to genome-encoded factors such as chaperones, a remarkable additional element, which is itself inherited in a non-Mendelian manner, regulates the de novo appearance of *[PSI$^+$]* (Derkatch et al., 1997, 2000). In yeast strains possessing the *[PSI$^+$]* inducibility factor (termed *[PIN$^+$]*), transient overexpression of the Sup35p prion domain leads to the appearance of *[PSI$^+$]* at a high frequency. In contrast, strains lacking the *[PIN$^+$]* factor (referred to as *[pin$^-$]*) do not convert to *[PSI$^+$]* upon Sup35p overexpression. Propagation of *[PIN$^+$]* does not depend on Sup35p and, like known yeast prions, *[PIN$^+$]* is inherited in a cytoplasmic manner, requires the presence of Hsp104p, and can be eliminated by treatment of cells with guanidine. Despite these arguments for a prion basis for *[PIN$^+$]*, the specific prion-forming protein

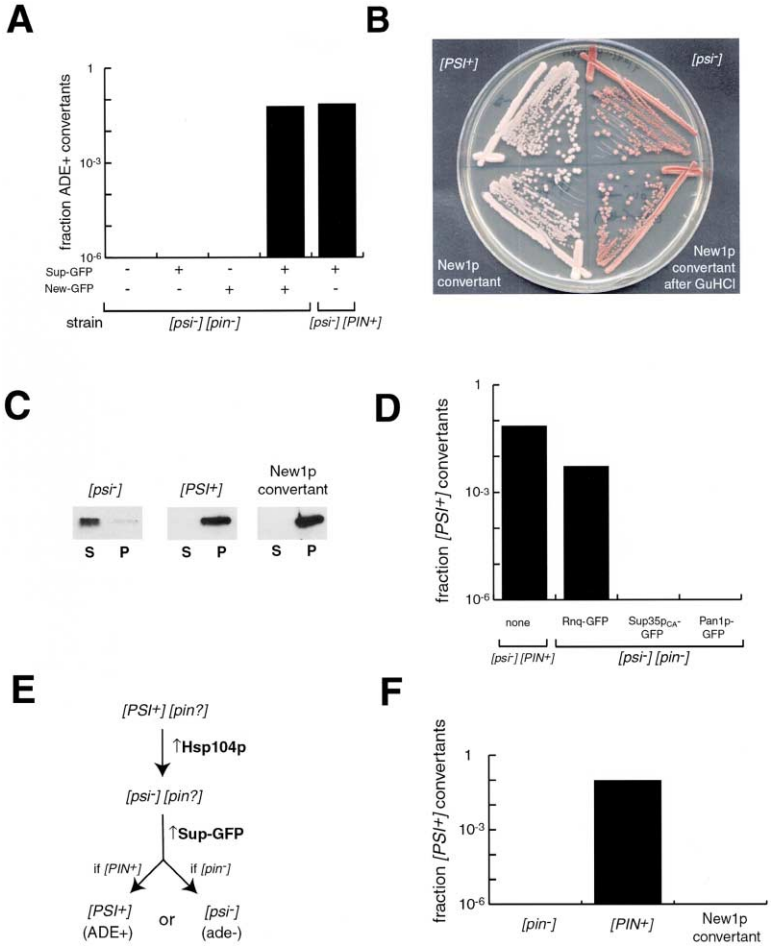

Figure 1. New1p and Rnq1p Prion Domains Facilitate Conversion to *[PSI$^+$]*

(A) New-GFP overexpression circumvents the requirement for *[PIN$^+$]* in *[PSI$^+$]* induction. The indicated proteins were overexpressed in a *[psi$^-$] [pin$^-$]* strain, and the frequency of conversion to ADE+ was determined by plating equal quantities of cells onto media with or without adenine. For comparison, a *[psi$^-$] [PIN$^+$]* control expressing Sup-GFP alone is shown. In these and subsequent prion induction experiments, each column represents the sum of 2–5 independent experiments in which 200–400 colonies were counted.

(B) Reversibility of ADE+ in New1p-mediated convertants. ADE+ convertants obtained by dual overexpression of Sup-GFP and New-GFP (New1p convertant) are shown before and after treatment with 5 mM guanidine hydrochloride (GuHCl) along with *[PSI$^+$]* and *[psi$^-$]* controls.

(C) Biochemical evidence that New1p-mediated convertants are *[PSI$^+$]*. Extracts from the indicated strains were subjected to ultracentrifugation; the presence of Sup35p in the supernatant (S) or pellet (P) was determined by immunoblotting after SDS-PAGE.

(D) Effect of other Gln/Asn-rich domains on *[PSI$^+$]* induction. Residues 153–415 of Rnq1p, 1–295 of Sup35p$_{CA}$, and 1–240 of Pan1p were fused to GFP and tested for *[PSI$^+$]* induction when overexpressed in a *[psi$^-$] [pin$^-$]* strain together with Sup-GFP. Sup-GFP alone in a *[psi$^-$] [PIN$^+$]* strain is shown at left. In all strains, overexpression of these proteins alone did not induce *[PSI$^+$]* (data not shown). The lower efficiency of *[PSI$^+$]* induction by Rnq-GFP compared to New-GFP is likely due to the lower propensity of Rnq-GFP to aggregate de novo in *[pin$^-$]* strains.

(E) Scheme for ascertaining the presence of *[PIN$^+$]* in New1p- and Rnq1p-mediated *[PSI$^+$]* convertants. The *[PSI$^+$]* factor is eliminated by overexpression of Hsp104p, then Sup-GFP is transiently overexpressed. If the strain is *[PIN$^+$]*, *[PSI$^+$]* should reappear (bottom left), whereas in *[pin$^-$]* strains, Sup-GFP overexpression should not induce *[PSI$^+$]* (bottom right).

(F) New1p-mediated *[PSI$^+$]* convertants are *[pin$^-$]*. We used the scheme in (E) to test for the presence of *[PIN$^+$]* in a New1p-mediated convertant. For comparison, conversion rates in *[pin$^-$]* and *[PIN$^+$]* strains are shown.

or proteins associated with the *[PIN$^+$]* state have remained mysterious.

We thus have two new prion proteins with unknown functions (New1p and Rnq1p) and an epigenetic prion-like phenomenon (*[PIN$^+$]*) without a known protein. Here, we establish that prion forms of both New1p and Rnq1p can promote *[PSI$^+$]* formation. The identification of *[PSI$^+$]*-inducing prions has allowed us to examine the mechanism of prion formation and to uncover a broader role for prions in modulating polyGln aggregation.

Results

Overexpression of Non-Sup35p Prion Domains Confers *[PSI$^+$]* Susceptibility

To test whether newly identified prions could, like *[PIN$^+$]*, act as *[PSI$^+$]*-promoting factors, we examined the effect of New1p aggregates on *[PSI$^+$]* induction. For these studies, we transiently overexpressed fusion proteins composed of either the New1p prion domain (residues 1–153) or the Sup35p prion domain (residues 1–253) and the green fluorescent protein, termed New-GFP and Sup-GFP, respectively. In contrast to Sup-GFP, which does not aggregate in *[pin$^-$]* strains, overexpressed New-GFP formed visible aggregates (see Figure 5D). We assayed for *[PSI$^+$]* induction by using strains with a nonsense mutation in the *ADE1* gene (*ade1-14*) that permits growth on medium lacking adenine (−ade) as a result of *[PSI$^+$]*-mediated nonsense suppression.

We found that overexpression of New-GFP circumvented the requirement for *[PIN$^+$]* in *[PSI$^+$]* induction. As expected, overexpression of New-GFP or Sup-GFP alone did not induce *[PSI$^+$]* in *[pin$^-$]* strains (conversion frequencies $<10^{-6}$, Figure 1A). However, overexpression of both Sup-GFP and New-GFP in a *[pin$^-$]* strain caused the appearance of adenine prototrophic (ADE+) colonies at a frequency ($\sim 6 \times 10^{-2}$) comparable to that occurring after overexpression of Sup-GFP alone in a *[PIN$^+$]* strain. We obtained similar results using full-length New1p in place of New-GFP (data not shown).

Several observations argued that these ADE+ convertants resulted from the de novo appearance of the *[PSI$^+$]* prion. First, they formed visible colonies after

Table 1. Genetic Analysis of New1- and Rnq1-Mediated *[PSI$^+$]* Induction

	Overexpressed Protein			Conversion to *[PSI$^+$]*		
	Sup-GFP	New-GFP	Rnq-GFP	wild-type	Δ*new1*†	Δ*rnq1*
[pin$^-$]	√			−	−	−
		√		−	−	−
			√	−	−	−
	√	√		++	++	++
	√		√	+	+	+
[PIN$^+$]	√			++	++	−*

[psi$^-$] strains of a *NEW1 RNQ1* (wild-type), Δ*new1* or Δ*rnq1* background over expressing the indicated GFP fusion proteins were assayed for conversion to *[PSI$^+$]* in the presence or absence of *[PIN$^+$]* by growth on −ade. — indicates no conversion to *[PSI$^+$]*, + indicates ~1% conversion and ++ represents ~10% conversion. All Δ*new1* experiments (†) showed delayed manifestation of *[PSI$^+$]*; colonies appeared on −ade after ~14 days, instead of the 5 days seen with wild-type strains.

* indicates permanent loss of the *[PIN$^+$]* factor; unlike their wild type sister spores, Δ*rnq1* haploids derived from a *[PIN$^+$]* Δ*rnq1*/+ diploid failed to manifest *[PIN$^+$]* as assayed by Sup-GFP aggregation and *[PSI$^+$]* induction and did not transmit *[PIN$^+$]* in subsequent back-crosses against *RNQ1 [pin$^-$]* strains.

approximately 5 days on −ade and displayed variable degrees of strength and stability of the ADE+ trait, features typical of fresh *[PSI$^+$]* inductants (Derkatch et al., 1996). Additionally, the ADE+ property of these convertants could be abolished by treatment with guanidine (Tuite et al., 1981), which cures all known yeast prions (Figure 1B). Finally, in extracts prepared from a New1p-converted strain, Sup35p fractionated entirely to the pellet following ultracentrifugation (Figure 1C), indicating that the ADE+ property of these strains arose from prion formation by Sup35p (Patino et al., 1996; Paushkin et al., 1996).

We tested whether other Gln/Asn-rich proteins could promote *[PSI$^+$]* induction by overexpressing GFP fusions of the prion domains of two other known prion-forming proteins, Rnq1p and *Candida albicans* Sup35p ($Sup35p_{CA}$) (Santoso et al., 2000; Sondheimer and Lindquist, 2000), as well as the Gln/Asn-rich portion of Pan1p. We saw varying levels of GFP aggregation in *[pin$^-$]* strains expressing each of these proteins alone. However, only the Rnq-GFP fusion promoted *[PSI$^+$]* induction, although at a lower frequency (5×10^{-3}) than did New-GFP (Figure 1D). Thus, only a subset of Gln/Asn-rich aggregates facilitate *[PSI$^+$]* induction.

The induction of *[PSI$^+$]* by dual overexpression of Sup-GFP and New-GFP could result from the conversion of the cells from *[pin$^-$]* to *[PIN$^+$]*, which would then permit *[PSI$^+$]* induction by excess Sup-GFP (Derkatch et al., 2000). However, when we eliminated the *[PSI$^+$]* factor from the New-GFP- or Rnq-GFP-mediated inductants using Hsp104p overexpression, a treatment which does not cure *[PIN$^+$]* (Derkatch et al., 1997), the resulting *[psi$^-$]* strains proved refractory to reinduction of *[PSI$^+$]* by overexpression of Sup-GFP alone (Figures 1E and 1F; data not shown), indicating that these strains had remained *[pin$^-$]*. Thus, New1p- and Rnq1p-mediated conversion from *[psi$^-$]* to *[PSI$^+$]* occurred without conversion to *[PIN$^+$]*.

[PSI$^+$] Susceptibility Does Not Arise from Inactivation of Chromosomally Encoded New1p and Rnq1p Proteins

To determine the roles of full-length New1p and Rnq1p in *[PSI$^+$]* induction, we deleted the corresponding genes and tested the effect of these mutations on the ability of Sup-GFP to induce *[PSI$^+$]*. We found that *[PSI$^+$]* inducibility arose from novel, gain-of-function properties of New-GFP and Rnq-GFP aggregates. Neither deletion of *NEW1* nor *RNQ1* rendered *[pin$^-$]* yeast susceptible to *[PSI$^+$]* induction by Sup-GFP alone (Table 1). Moreover, *[PSI$^+$]* induction by dual overexpression of Sup-GFP together with New-GFP or Rnq-GFP still occurred in these deletion strains. Thus, New1p- and Rnq1p-mediated *[PSI$^+$]* induction does not arise from loss of the activity of their corresponding full-length proteins. In contrast, deletion of *RNQ1* prevented the manifestation and propagation of the classical *[PIN$^+$]* factor, a finding consistent with the identification of Rnq1p as the protein determinant of *[PIN$^+$]* (Derkatch et. al, 2001 [this issue of *Cell*]). In Δ*new1* strains, there was a significant delay in the onset of the *[PSI$^+$]* phenotype regardless of whether *[PSI$^+$]* induction was promoted by New-GFP, Rnq-GFP, or *[PIN$^+$]* (Table 1 and data not shown). Once converted, *[PSI$^+$]* Δ*new1* strains grew at a normal rate, suggesting that the chromosomally-encoded New1p assists in the induction but not propagation of *[PSI$^+$]*.

Aggregation of New1p NYN Repeats Is Needed for *[PSI$^+$]* Induction

We next constructed a panel of truncated New1p-GFP fusions in order to investigate the relationship between the aggregation of New1p and its ability to promote *[PSI$^+$]* induction. The prion domain of New1p contains a particularly Gln/Asn-rich region between residues 50 and 100. Notably, residues 62-70 (QQGGYQSYN) resemble an oligopeptide repeat found in Sup35p (PQGGYQ-QYN) that influences the stability and severity of *[PSI$^+$]* (Liu and Lindquist, 1999), while residues 71–100 of New1p contain the repeating tripeptide sequence NYN (Figure 2A).

We found that an intact NYN-rich region is essential for both New1p aggregation and its ability to promote *[PSI$^+$]* induction (Figure 2B), whereas other portions of the New1p prion domain proved unnecessary for either effect. The C-terminal GFP domain was not required for *[PSI$^+$]* inducibility, as overexpression of an EE epitope-tagged version of the NYN region also promoted *[PSI$^+$]* formation. Replacement of the first or third asparagine pairs of the NYN motif with large, positively charged residues (arginines) decreased both aggregation and

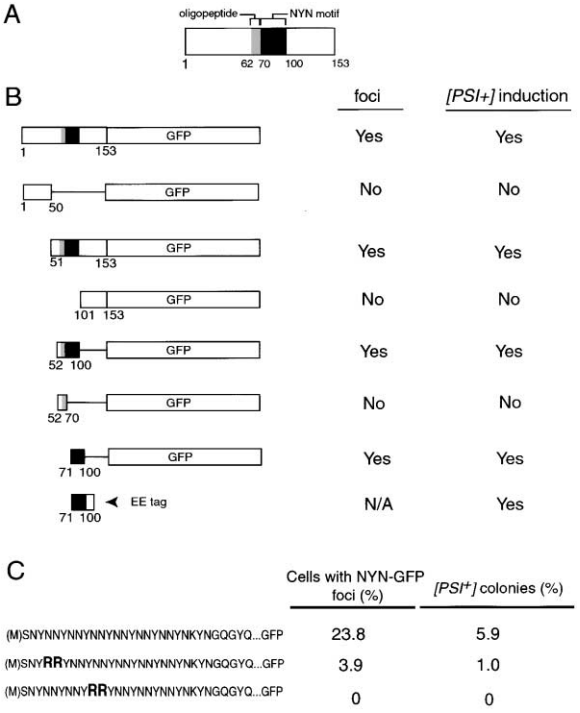

Figure 2. Mutational Analysis Reveals a Relationship between New1p Aggregation and [PSI$^+$] Induction

(A) A schematic diagram of the New1p prion domain (residues 1–153). The oligopeptide region similar to Sup35p (QQGGYQSYN, residues 62–70, gray) and the NYN repeat motif (residues 70–100, black) are indicated.

(B) NYN motif of New1p confers both aggregation and *[PSI$^+$]* inducibility. Fusions between the indicated regions of New1p and GFP were assayed for focus formation (visualized by fluorescent microscopy) when overexpressed alone, as well as the ability to facilitate *[PSI$^+$]* induction when overexpressed along with Sup-GFP. The New$_{70\text{-}100}$-EE construct was approximately 10 times less effective than the New-GFP construct at inducing *[PSI$^+$]* in conjunction with Sup-GFP, possibly due to poor expression.

(C) Disruption of the NYN motif affects aggregation and *[PSI$^+$]* inducibility. Pairs of arginines (denoted RR) were introduced in place of asparagine pairs at the indicated positions in the NYN tract of New1$_{70\text{-}100}$-GFP. The percentage of cells containing visible GFP inclusions and cells converted to *[PSI$^+$]* are shown.

conversion to *[PSI$^+$]* (Figure 2C). Compared to an unmutated control, the distal arginine mutations diminished both the fraction of cells with aggregates and the rate of *[PSI$^+$]* induction roughly 6-fold; introduction of arginine residues near the center of the NYN motif completely abolished both the aggregation and *[PSI$^+$]*-promoting properties of New1p. These data argue that susceptibility to *[PSI$^+$]* induction arises from aggregation of New1p via its NYN repeat motif.

The *[NU$^+$]* Prion Confers Susceptibility to *[PSI$^+$]* Induction

The preceding experiments linked *[PSI$^+$]* inducibility to the presence of New-GFP aggregates produced by overexpression. We asked whether low levels of a constitutively aggregated form of the New1p prion domain could also confer *[PSI$^+$]* inducibility. To generate pure populations of cells containing such aggregates without a need for continuous New-GFP overexpression, we replaced the chromosomal copy of *SUP35* with an episomal gene encoding a fusion of the New1p prion domain and the essential translation termination domain of Sup35p. In the resulting strains, this protein (termed New-EF) could be interconverted from a soluble *[nu$^-$]* form to the self-propagating aggregated state, *[NU$^+$]* (Santoso et al., 2000). In *[NU$^+$]* strains, the majority of chromosomally encoded New1p protein is also aggregated (data not shown). As with *[PSI$^+$]*, the *[NU$^+$]* state could be monitored phenotypically by nonsense suppression of *ade1-14*, resulting in adenine prototrophy.

We first established the prion nature of New-EF aggregates responsible for *[NU$^+$]*. As with other yeast prions, transient treatment of *[NU$^+$]* cells with guanidine caused efficient reversion to the *[nu$^-$]* state (Figure 3A). Similarly, we were unable to obtain *[NU$^+$]* isolates in strains lacking Hsp104p, which is thought to be the target of guanidine (Jung and Masison, 2001) (data not shown). New-EF protein is required for the propagation of *[NU$^+$]*, as transient loss of the New-EF-expressing plasmid caused reversion to *[nu$^-$]* (Figure 3B). Finally, *[NU$^+$]* can be transmitted in an "infectious" manner through cytoplasmic transfer (cytoduction) from *[NU$^+$]* cells to karyogamy-defective *[nu$^-$]* cells (Figure 3C). Whereas *[NU$^+$]* donors efficiently transferred adenine prototrophy to *[nu$^-$]* recipients, no ADE+ colonies were obtained when *[nu$^-$]* donors were used. Combined with previously published data (Santoso et al., 2000), these results confirmed that *[NU$^+$]* results from an infectious, reversible, conformational isoform (i.e., prion) of the New-EF protein.

We next created a panel of strains that harbored one, both, or neither of the *[PIN$^+$]* or *[NU$^+$]* prions and used fluorescence microscopy to monitor the formation of Sup-GFP aggregates, which appeared as both foci and "ribbons" (Figure 4A). Although it is unknown whether these structures are active *[PSI$^+$]* seeds, their formation depends on the induction or presence of *[PSI$^+$]* and thus serves as an indicator of *[PSI$^+$]* susceptibility (Patino et al., 1996; Zhou et al., 2001).

We found that *[NU$^+$]* conferred susceptibility to *[PSI$^+$]* induction in a manner that was comparable to but independent of *[PIN$^+$]*. *[NU$^+$]* alone promoted the appearance of Sup-GFP foci at an efficiency somewhat higher than *[PIN$^+$]* alone, and in combination, *[NU$^+$]* and *[PIN$^+$]* resulted in a further increase in the formation of foci (Figure 4B). By contrast, no Sup-GFP aggregates were seen in cells lacking both prion elements, including *[NU$^+$] [pin$^-$]* strains that spontaneously reverted to *[nu$^-$] [pin$^-$]* (Figure 4B and data not shown). We directly demonstrated the presence of prion seeds in cells with such Sup-GFP aggregates by using them to seed the conversion of full-length Sup35p to a *[PSI$^+$]* state. We first accumulated Sup-GFP aggregates in Δ*sup35* strains, then exposed these aggregates to full-length Sup35p through mating with a *[psi$^-$] [pin$^-$]* strain with an intact *SUP35* gene (depicted in Figure 4C); the resulting diploids were assayed for conversion to *[PSI$^+$]*. Only donor strains with visible Sup-GFP aggregates prior to mating (i.e, strains with either the *[NU$^+$]* or *[PIN$^+$]* prions) yielded *[PSI$^+$]* diploid colonies (Figure 4D). Taken together, these findings establish that prion-facilitated *[PSI$^+$]* inducibility can arise from the presence of multiple independent prions.

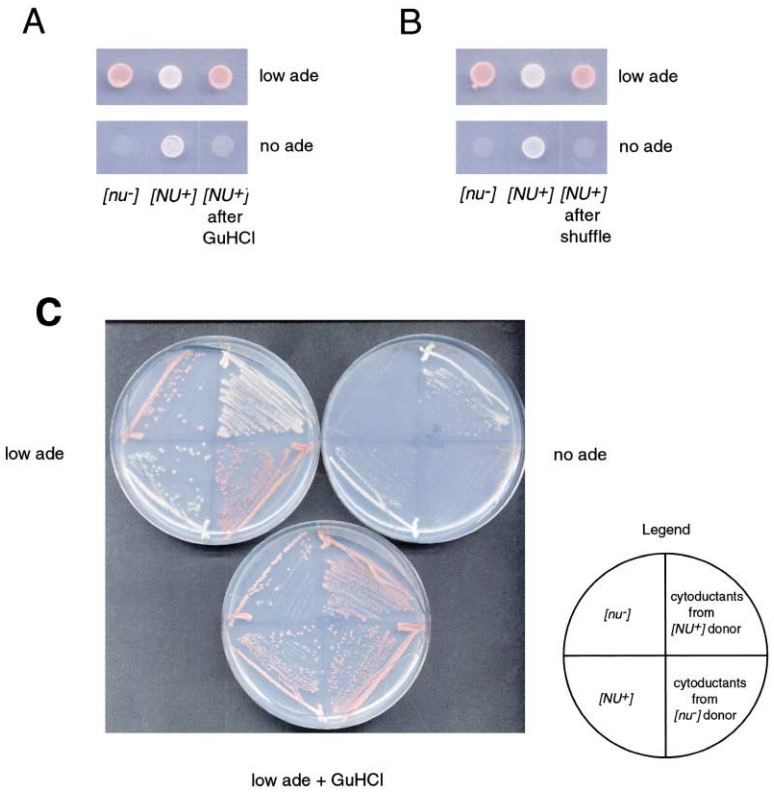

Figure 3. *[NU$^+$]* Is a Prion Form of New-EF

(A) *[NU$^+$]* is eliminated by guanidine treatment. Shown are spotted cultures of *[nu$^-$]* and *[NU$^+$]* strains and the *[NU$^+$]* strain after transient growth (approximately 20 generations) in the presence of guanidine. The strains shown here and in subsequent panels are *[PIN$^+$]*, but similar results were obtained with *[pin$^-$]* derivatives.

(B) Propagation of *[NU$^+$]* requires the continuous expression of the New-EF protein. *[NU$^+$]* strains bearing an episomal copy of New-EF were transformed with a plasmid encoding Sup35p and were allowed to lose the New-EF plasmid. These isolates were then retransformed with the New-EF plasmid and were allowed to lose the *SUP35* plasmid. When tested for *ade1-14* nonsense suppression after this plasmid "shuffle," the resulting strains had lost the *[NU$^+$]* trait.

(C) *[NU$^+$]* is efficiently transmitted by cytoplasmic transfer (cytoduction). Cytoductants from *[nu$^-$]* or *[NU$^+$]* donor strains to a karyogamy-deficient *[nu$^-$]* recipient are shown growing on media with low or no adenine (top). Cytoductable adenine prototrophy was abolished by growth on medium with guanidine (bottom), confirming its prion basis. Shown are streaks from nonclonal cytoductant patches; when individual cytoductant colonies were scored for *[NU$^+$]*, 17 of 17 colonies obtained using a *[NU$^+$]* donor had become *[NU$^+$]*, while 17 of 17 colonies from *[nu$^-$]* donor remained *[nu$^-$]*. For comparison, the *[NU$^+$]* and *[nu$^-$]* donor stains are also shown.

New1p Aggregates Do Not Appear to Seed Sup35p Polymerization

New1p or Rnq1p prions could promote *[PSI$^+$]* induction by providing a nucleating seed into which Sup35p could become incorporated. However, several experiments designed to detect such cross-seeding yielded negative results. First, New-GFP overexpression did not by itself stimulate *[PSI$^+$]* induction, even in an already susceptible *[PIN$^+$]* strain (Figures 1A and 5A). Conversely, Sup35p aggregates produced by overexpressing Sup-GFP in a *[PIN$^+$]* strain did not increase the rate of appearance of *[NU$^+$]* (Figure 5B). Additionally, overexpression of Sup35p did not induce *[PIN$^+$]* (Derkatch et al., 1997). Finally, the presence of purified recombinant New1p prion domain did not affect the kinetics of Sup35p prion domain polymerization in vitro (data not shown).

To test directly for cross-interaction between Sup35p and New1p prion domains in vivo, we examined the localization of these proteins in the same cells using two-color fluorescence microscopy. A fusion of the Sup35p prion domain with yellow fluorescent protein (Sup-YFP) displayed diffuse cytoplasmic localization when overexpressed alone in a *[pin$^-$]* strain (Figure 5C); in contrast, a New1p prion domain–cyan fluorescent protein fusion (New-CFP) formed aggregates when overexpressed alone in the same strain (Figure 5D). When these proteins were overexpressed together, 2%–5% of the cells displayed aggregates of Sup-YFP (Figure 5E) as well as of New-CFP, but these two types of inclusions did not colocalize (Figure 5F). Thus, the presence of New-CFP permitted the ordinarily soluble Sup-YFP to aggregate, but not into the same inclusions as New-CFP.

The Role of Chaperones in *[PSI$^+$]* Induction

Another possible basis for New1p-mediated *[PSI$^+$]* induction might involve changes in the activities of chaperones that modulate *[PSI$^+$]*. The presence of aggregated New1p could in principle elevate Hsp104p activity, which has been suggested to stimulate the folding of the *[PSI$^+$]* form of Sup35p. However, we found that New-CFP promoted Sup-YFP aggregation even in the absence of Hsp104p. In a strain lacking Hsp104p, Sup-YFP displayed diffuse localization when overexpressed alone (Figure 6A), while New-CFP formed aggregates (Figure 6B) similar to those seen in wild-type controls (Figure 5D). As in wild-type cells, the presence of New-CFP permitted Sup-YFP to aggregate (Figure 6C). Overexpression of chaperones also did not prevent New-GFP from stimulating *[PSI$^+$]* induction. We expressed New-GFP and Sup-GFP in a strain bearing a high-copy *HSP104* plasmid previously shown to cure *[PSI$^+$]*, but this did not have a substantial effect on the ability of New-GFP to promote *[PSI$^+$]* induction (Figure 6D). We performed similar experiments with high-copy plasmids encoding Ssa1p and Ssb1p, two Hsp70 proteins known to affect *[PSI$^+$]* formation (Chernoff et al., 1999; Newnam et al., 1999), and obtained similar results

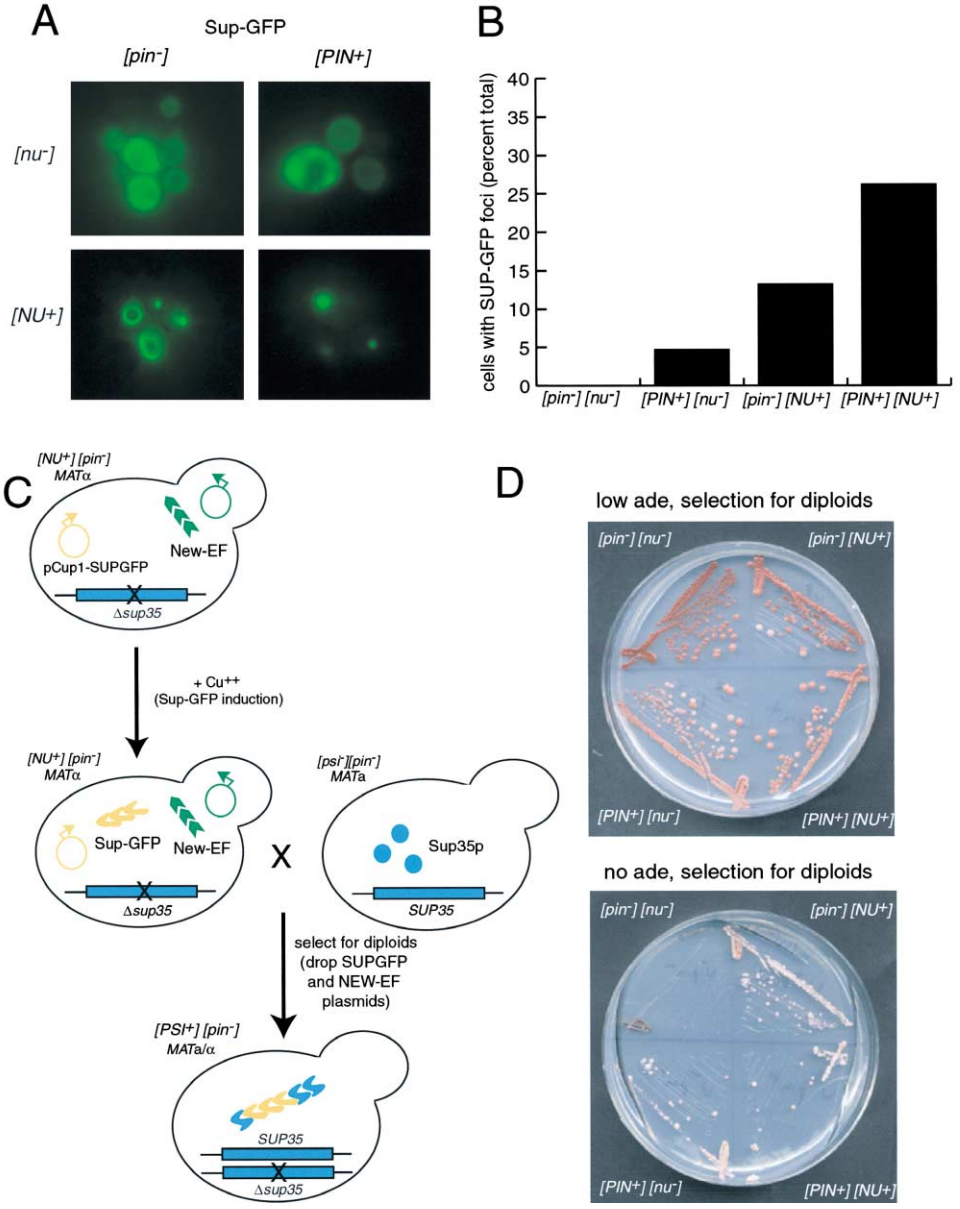

Figure 4. *[NU$^+$]* Confers Susceptibility to *[PSI$^+$]* Induction

(A) Sup-GFP forms aggregates in *[PIN$^+$]* or *[NU$^+$]* cells. Sup-GFP was expressed from a copper-inducible, high-copy plasmid in strains harboring neither, one, or both of the *[PIN$^+$]* and *[NU$^+$]* prions, as indicated. After 48 hr of expression, foci and ribbons of fluorescence were visible in cells harboring at least one prion. In this and subsequent fluorescence localization experiments (all of which were performed under similar conditions), ~50% of cells had little or no detectable fluorescence; nonfluorescent cells were nonetheless included in all quantitative analyses.

(B) Frequency of Sup-GFP focus formation in cells treated as described in (A).

(C) Scheme for testing the ability of preformed Sup-GFP aggregates to seed prion conversion of full-length Sup35p. Chromosomal *SUP35* (blue) was disrupted, allowing *[NU$^+$]* to be monitored by inactivation of the New-EF protein (green). Aggregates of Sup-GFP (orange) were accumulated by copper-induced overexpression from the pCup1-SUPGFP plasmid (top left). The cells were then mated with a *[psi$^-$] [pin$^-$]* strain expressing full-length Sup35p (middle). The *[PSI$^+$]* state of the resulting diploid was assayed by growth on −ade. The appearance of *[PSI$^+$]* indicated that Sup-GFP aggregates had seeded the prion conversion of full-length Sup35p (bottom). Similar experiments were performed starting with cells lacking *[PSI$^+$]*-promoting prions, with *[PIN$^+$]* alone or with both *[NU$^+$]* and *[PIN$^+$]*. In all cases, diploids were plated on medium that allowed the loss of the Sup-GFP- and New-EF-encoding plasmids.

(D) Demonstration that Sup-GFP aggregates formed as a result of the presence of *[NU$^+$]* and *[PIN$^+$]* can seed *[PSI$^+$]* induction. Cells with neither, one, or both of the *[PIN$^+$]* and *[NU$^+$]* prions were treated as described in (C). The top panel (low ade) shows the growth of all diploids, while the bottom panel (no ade) shows the growth of *[PSI$^+$]* diploids only. Note lack of growth in top left quadrant of bottom panel.

(data not shown). These observations indicate that the effect of New1p aggregates is not mitigated by altering levels of chaperones known to modulate *[PSI$^+$]*. Furthermore, they suggest that Hsp104p, which is absolutely required for the propagation of *[PSI$^+$]*, is not needed for the de novo formation of Sup35p aggregates.

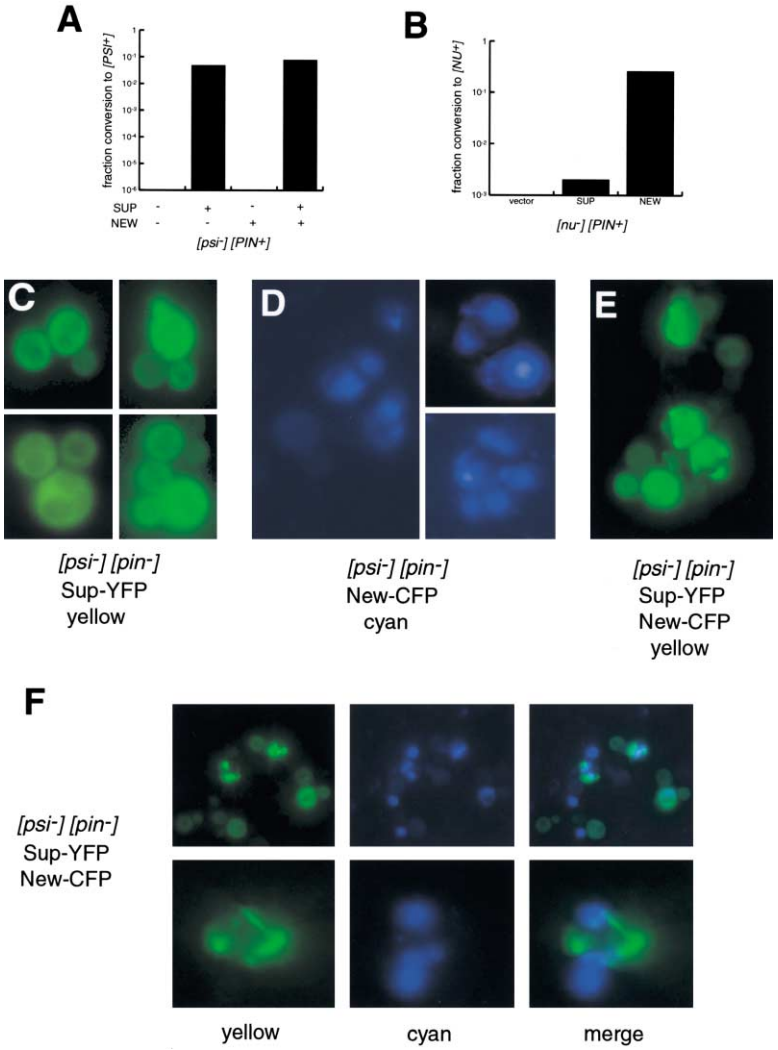

Figure 5. Lack of Cross-Interaction between New-GFP and Sup-GFP

(A) New-GFP aggregates do not induce *[PSI$^+$]*. The indicated GFP fusion proteins were overexpressed in a *[psi$^-$] [PIN$^+$]* strain and the frequency of conversion to *[PSI$^+$]* was determined as in Figure 1A.

(B) Sup-GFP aggregates do not induce *[NU$^+$]*. The indicated GFP fusion proteins were overexpressed in a *[nu$^-$] [PIN$^+$]* strain. Conversion to *[NU$^+$]* was monitored by nonsense suppression resulting from aggregation of New-EF protein. Note that the spontaneous frequency of appearance of *[NU$^+$]* is $\sim 10^{-3}$, significantly higher than that of *[PSI$^+$]*.

(C) Sup-YFP overexpressed alone in a *[psi$^-$] [pin$^-$]* strain displays diffuse localization. In these and subsequent micrographs, the prion status, expressed proteins, and the fluorescent light channel are indicated.

(D) New-CFP forms aggregates when overexpressed in *[psi$^-$] [pin$^-$]* strains. The majority of cells with visible fluorescence had inclusions, as shown here.

(E) Sup-YFP forms filamentous aggregates in a subset of cells when overexpressed together with New-CFP in a *[psi$^-$] [pin$^-$]* strain.

(F) New-CFP and Sup-YFP aggregates do not colocalize. A field view with yellow, cyan, and merged channels is shown at top, while the bottom row shows a magnified view from a separate experiment. In all cells with Sup-YFP inclusions, New-CFP inclusions were also observed. Lack of colocalization was confirmed by 3D reconstruction of wide-field microscopic images (O. Weiner and L.Z.O., data not shown).

Note: higher quality versions of this and other figures are available electronically at http://www.ucsf.edu/jswlab/downloads

[PSI$^+$] Inducibility Factors Promote polyGln Aggregation in Yeast

Finally, we asked whether the presence of *[PSI$^+$]*-promoting prions affected the aggregation of Gln/Asn-rich proteins other than Sup35p. We constructed GFP fusions of normal and glutamine-expanded variants of a fragment of the spinocerebellar ataxia type 3/Machado-Joseph Disease (MJD) protein (Ikeda et al., 1996) and overexpressed them in *[pin$^-$]* and *[PIN$^+$]* yeast. As expected, fusions with 22 glutamines (Q22-GFP) did not aggregate in either strain. In contrast, a fusion containing a pathogenic number of glutamines (Q62-GFP) formed visible foci, but the number and nature of these aggregates was greatly altered by the presence of *[PIN$^+$]* (Figures 7A–7C). In strains in which *[PIN$^+$]* had been eliminated by guanidine treatment or deletion of *HSP104*, Q62-GFP fluorescence was predominantly diffuse, with some cells ($\sim$6%) exhibiting a single large inclusion (Figure 7A top right); cells containing multiple foci were very rare ($\sim$1%). However, in a *[PIN$^+$]* strain, there were few cells with bright diffuse fluorescence; cells with visible aggregates were more abundant ($\sim$28%) and most of these cells ($\sim$18% of total) exhibited multiple minute foci (Figure 7A bottom right). We obtained similar results with a MJD protein-GFP fusion containing 82 glutamines (data not shown). Biochemical analysis confirmed that the *[PIN$^+$]* element promoted the aggregation of Q62-GFP, as this protein was depleted by ultracentrifugation from the supernatant of *[PIN$^+$]* but not *[pin$^-$]* extracts (Figure 7B). Like *[PIN$^+$]*, *[NU$^+$]* stimulated the appearance of multiple fluorescent foci of Q62-GFP (Figures 7C and 7D). However, *[PSI$^+$]* did not promote the formation of Q62-GFP foci (Figure 7C). Together, these observations reveal a role for *[PSI$^+$]*-promoting prions in the general regulation of protein aggregation and suggest a common mechanism for the initiation of Sup35p and polyGln disease protein aggregates.

Discussion

Susceptibility to induction of the yeast *[PSI$^+$]* prion has previously been shown to require a non-Mendelian element, *[PIN$^+$]*, which itself propagates in a prion-like manner (Derkatch et al., 1997, 2000). We have investigated the role of two Gln/Asn-rich prion domains, those of New1p and Rnq1p, in the process of *[PSI$^+$]* induction. Our studies reveal that the prion forms of these proteins control not only susceptibility to *[PSI$^+$]* formation but

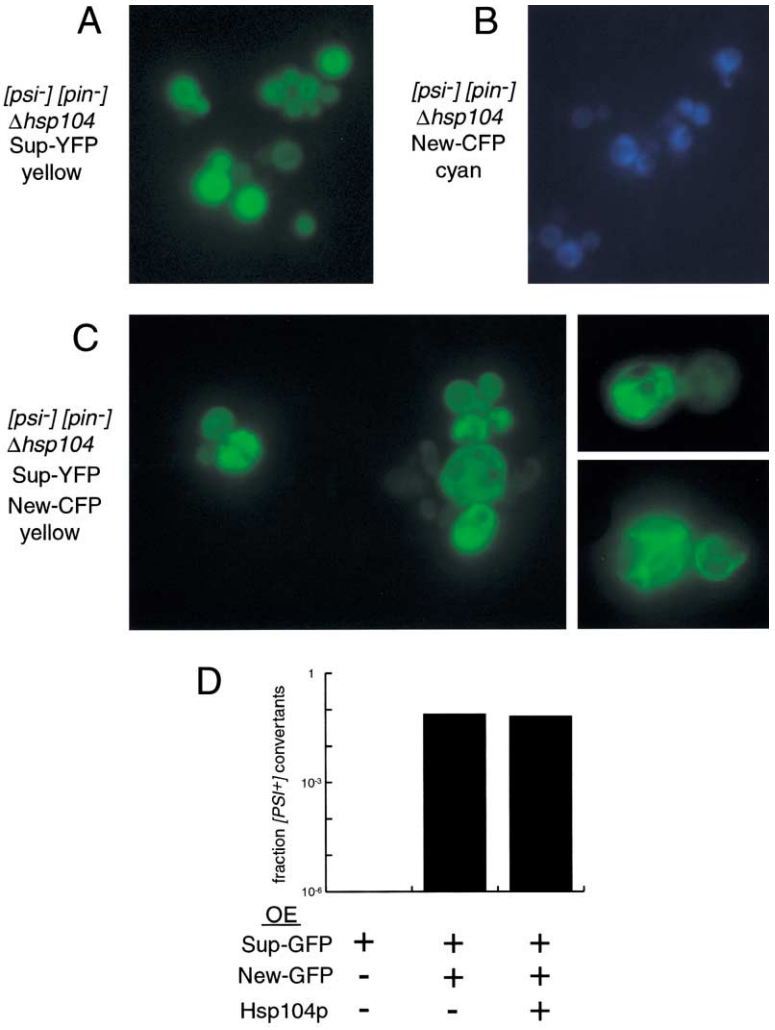

Figure 6. Altered Hsp104p Levels Do Not Affect New1-Mediated Sup35p Aggregation or *[PSI$^+$]* Induction

(A) Examples of the diffuse localization of Sup-YFP observed in a Δ*hsp104* strain in the absence of New-CFP overexpression.

(B) Examples of New-CFP aggregates in a Δ*hsp104* strain.

(C) New-CFP-mediated aggregation of Sup-YFP does not require Hsp104p. A *[psi$^-$] [pin$^-$]* Δ*hsp104* strain overexpressing both Sup-YFP and New-CFP displayed Sup-YFP inclusions at a frequency (~2%) similar to that in *[psi$^-$] [pin$^-$]* cells with intact *HSP104* (see Figure 5E).

(D) Hsp104p overexpression does not affect New1p-mediated *[PSI$^+$]* induction. *[psi$^-$] [pin$^-$]* strains with or without a high-copy *HSP104* plasmid were plated onto −ade after overexpression of the indicated GFP fusion proteins. When these strains were plated onto −ade while still selecting for the *HSP104* plasmid, no ADE+ colonies were observed, confirming that overexpressed *HSP104* could prevent *[PSI$^+$]* propagation (data not shown).

also enhance the aggregation of a fragment of a human disease protein (MJD) containing a pathogenic number of glutamine repeats. Additionally, we have described a novel mode of yeast prion action that, as with the mammalian prions, arises from gain-of-function properties of protein aggregates rather than from the inactivation of the normal protein (Prusiner, 1998; Wickner et al., 1999).

We have established that while susceptibility to *[PSI$^+$]* induction can be conferred by at least two yeast prion domains, it is not an obligatory consequence of the accumulation of intracellular Gln/Asn-rich aggregates. *[PSI$^+$]* inducibility is widespread among laboratory yeast strains (L.Z.O. and J.S.W., unpublished data), as is the presence of Rnq1p aggregates (Sondheimer and Lindquist, 2000); indeed, an accompanying paper demonstrates that the prion form of Rnq1p is responsible for the classical *[PIN$^+$]* state (Derkatch et al., 2001 [this issue of *Cell*]). Given the large number of other potential prions in the yeast genome (Michelitsch and Weissman, 2000), it seems likely that additional, as-yet-undiscovered prions will also confer susceptibility to *[PSI$^+$]* induction.

Several observations suggest a common mechanism of action by the prion forms of New-EF (*[NU$^+$]*) and Rnq1p (*[PIN$^+$]*). Both prions render the cell susceptible to *[PSI$^+$]* induction and enhance polyGln aggregation. Furthermore, *[PSI$^+$]* susceptibility arising from either prion is partially compromised by deletion of the chromosomal *NEW1* gene. Finally, Sup-GFP aggregates generated by virtue of *[NU$^+$]* and *[PIN$^+$]* are microscopically indistinguishable and lead to a similar range of *[PSI$^+$]* prion "strains" (Derkatch et al., 1996).

A Saturable Antiaggregation System?

How do aggregates of New1p or Rnq1p make cells vulnerable to *[PSI$^+$]* induction? Our findings exclude several models. First, *[PSI$^+$]* induction does not occur as a result of the de novo appearance of the *[PIN$^+$]* factor. Second, *[PSI$^+$]* induction does not arise through loss of functional New1p or Rnq1p; deletion of these genes did not confer *[PSI$^+$]* inducibility. Third, New1p-mediated *[PSI$^+$]* susceptibility is not solely caused by changes in Hsp104p activity, as neither loss nor overexpression of Hsp104p modulated this phenomenon.

[PSI$^+$] susceptibility could arise from cross-seeding between aggregates of Sup35p and those of New1p and Rnq1p prion domains. However, several observations

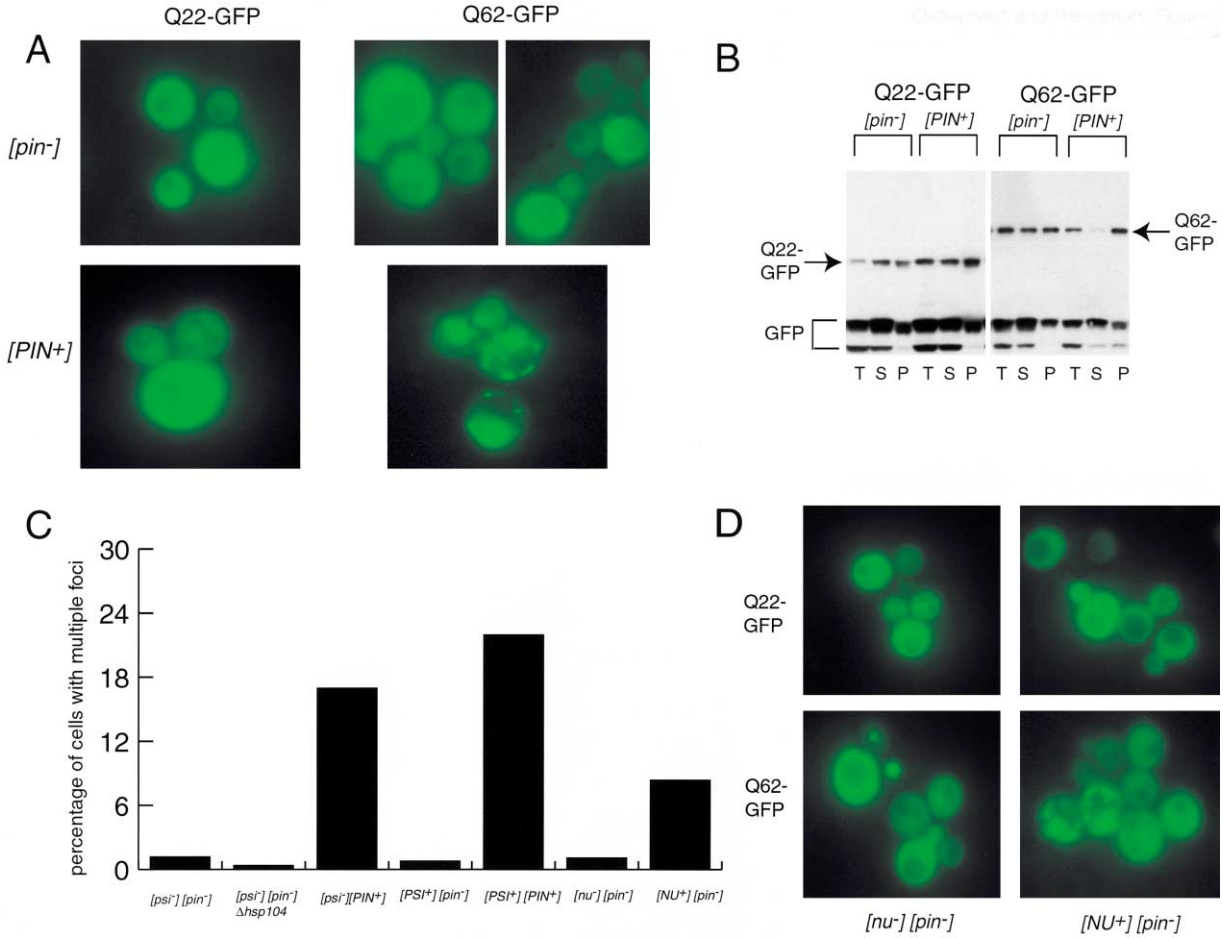

Figure 7. *[PIN$^+$]* and *[NU$^+$]* Promote Aggregation of the polyGln Disease Protein MJD/ataxin-3

Q22 and Q62 refer to MJD protein-GFP fusions containing 22 and 62 Gln residues, respectively.

(A) Representative fluorescence micrographs illustrating the effect of glutamine repeat length and the *[PIN$^+$]* prion on MJD-GFP aggregation. Q22 and Q62 were overexpressed in *[psi$^-$] [pin$^-$]* and *[psi$^-$] [PIN$^+$]* strains. Note the single large inclusion (top right) seen in a subset of *[pin$^-$]* Q62 cells; in contrast, *[PIN$^+$]* Q62 cells displayed more abundant multiple aggregates (bottom right).

(B) Centrifugation analysis of MJD-GFP. Lysates prepared from the indicated strains overexpressing either Q22 or Q62 were subjected to ultracentrifugation and the total (T), supernatant (S), and pellet (P) fractions were analyzed by SDS-PAGE followed by immunoblotting with α-GFP. Q22 is distributed equally between the supernatant and the pellet in both strains, while Q62 sediments almost entirely to the pellet of the *[PIN$^+$]* extract but remains soluble in the *[pin$^-$]* extract. The smaller bands (GFP) likely result from proteolytic removal of the MJD region; as expected, these fragments are not depleted from the supernatant.

(C) Effect of various yeast prions on Q62 aggregation. For each of the indicated strains, the fraction of cells with multiple fluorescent foci was determined as in Figure 3A. The lower stimulation of aggregation of Q62 by *[NU$^+$]* compared to *[PIN$^+$]* may result from the rapid reversion of these strains to *[nu$^-$]* under these conditions (data not shown). Note that *[PSI$^+$]* does not stimulate Q62 aggregation.

(D) Representative *[nu$^-$] [pin$^-$]* and *[NU$^+$] [pin$^-$]* cells overexpressing Q22 and Q62.

argue against this model. Sup35p prion propagation is typically self-specific; even single amino acid changes can prevent cross-seeding between wild-type and mutant Sup35p proteins (DePace et al., 1998). While a small portion of New1p does resemble an oligopeptide repeat sequence found in Sup35p, this region proved dispensable for *[PSI$^+$]* induction. Furthermore, New-GFP overexpression alone failed to induce *[PSI$^+$]*, and Sup35p overexpression did not stimulate *[NU$^+$]* induction. Finally, Sup-YFP and New-CFP aggregates in the same cell did not colocalize. Despite these findings, it remains possible that some cross-seeding could occur at a low level, and we are unable to conclusively rule out such a basis for the observed phenomena.

As an alternative model, we suggest that there may exist saturable cellular factors that antagonize de novo formation of prion-like aggregates. In a prion-free (*[psi$^-$] [pin$^-$]*) strain, overexpressed Sup35p could be recognized by these antiaggregation factors and prevented from aggregating. Aggregates of Rnq1p or New1p, whether arising from overexpression or the presence of heritable prions, could specifically inhibit this antiaggregation factor, thereby allowing Sup35p to form the *[PSI$^+$]* prion.

Chaperones and proteases can inhibit protein aggregation (Kopito, 2000), and are thus attractive candidates for saturation by *[PSI$^+$]*-promoting factors. Although overexpression of several chaperones known to affect *[PSI$^+$]* propagation did not appear to influence *[PSI$^+$]*

induction, multiple chaperones may be simultaneously inhibited by *[PSI$^+$]*-promoting prions. For example, it has been shown that Rnq1p aggregates interact with an Hsp40/Hsp70 protein pair (Sis1p and Ssa1p) (Sondheimer et al., 2001). Alternatively, degradation of aggregation-prone proteins by cellular proteases could be inhibited by prion-promoting aggregates; polyGln-rich aggregates have in fact been recently found to saturate the proteasome (Bence et al., 2001). Preliminary data suggest that Sup-GFP is subject to amino-terminal proteolytic processing, but overexpression of New-GFP or the presence of *[PIN$^+$]* antagonizes this effect (L.Z.O. and J.S.W., unpublished data). This inhibition of proteolysis occurs even with a mutant Sup-GFP (DePace et al., 1998) that does not aggregate, arguing that this protection from proteolysis is not merely a consequence of Sup35p aggregation.

Our findings also shed light on the role of Hsp104p in the induction and maintenance of *[PSI$^+$]*. To explain the dependence of *[PSI$^+$]* on Hsp104p, two models (which are not mutually exclusive) have been proposed. Hsp104p could assist the folding of Sup35p into an aggregation-competent state required for *[PSI$^+$]* formation (Patino et al., 1996). Alternatively, the dissaggregation activity of Hsp104p may be needed to split up Sup35p aggregates to allow efficient distribution of the prion to daughter cells in cell division (Kushnirov and Ter-Avanesyan, 1998). Because deletion of *HSP104* eliminates all known yeast prions including *[PIN$^+$]*, it has hitherto been impossible to determine whether Hsp104p is needed for the formation of Sup35p prion aggregates. However, overexpression of New1p circumvents the requirement for *[PIN$^+$]* in *[PSI$^+$]* induction, allowing us to test the effect of *HSP104* deletion on de novo Sup35p aggregation. We found that Sup-YFP in cells with aggregated New-CFP forms visible inclusions of similar appearance and frequency in both Δ*hsp104* and wild-type strains, demonstrating that Hsp104p is not needed for Sup35p aggregation per se. However, because Hsp104p is required for propagation of *[PSI$^+$]*, we were not able to directly test whether these aggregates were prions.

Implications for Human polyGln Protein Aggregation

A set of neurodegenerative diseases, including spinocerebellar ataxia type 3/Machado-Joseph Disease (MJD) and Huntington's Disease, result from the expansion of glutamine repeats that cause the affected proteins to form intracellular inclusions. We have found that, in yeast, the *[PIN$^+$]* and *[NU$^+$]* prions strongly modulate the aggregation of a fragment of the MJD protein bearing pathogenic glutamine tracts. Recently, it was demonstrated that deletion of *HSP104* abolishes the aggregation of glutamine-expanded Huntington's Disease protein in a yeast model (Krobitsch and Lindquist, 2000). Our results suggest that this requirement for *HSP104* may in part reflect the role of this chaperone in the maintenance of *[PIN$^+$]* or possibly other unidentified prions that promote polyGln aggregation.

The stimulation of MJD protein aggregation by *[PIN$^+$]* and *[NU$^+$]* establishes that the aggregation-promoting effect of these prions is not idiosyncratic to Sup35p but rather that they can also enhance the formation of polyGln aggregates, which are not known to be prion-like in character. A surprisingly large number of Gln/Asn-rich domains (~1% of total genomic ORFS) are encoded by eukaryotic genomes (Michelitsch and Weissman, 2000). Given the tendency of proteins of this type to aggregate, it is likely that cells seek to prevent such potentially deleterious misfolding. Differences in the level of antiaggregation activity from one cell type to another could contribute to the tissue specificity of polyGln diseases. Pathogenic aggregates may develop spontaneously in cells with a lower capacity to inhibit the initiation of polyGln aggregates. Once established, Gln/Asn-rich aggregates are likely to be difficult to eliminate and could tax the cell's ability to prevent other proteins from aggregating. Further studies of the initiation of aggregation in yeast and higher eukaryotes may thus prove fruitful in the identification of targets for prophylaxis against aggregation-based neurodegenerative diseases.

Experimental Procedures

Yeast Strains and Methods

Strains: *[PSI$^+$]* and *ade1-14* were introduced into W303 yeast by mating against the strain 74D-694a (Chernoff et al., 1995), followed by four backcrosses against the W303 parent, ultimately producing YJW 508 (*[PSI$^+$] [PIN$^+$] MAT*α, *ade1-14*, *his3-11,15*, *leu2-3*, *trp1-1*, *ura3-1*). YJW 509, the *[psi$^-$] [pin$^-$]* derivative of this strain, was obtained by growth of YJW 508 on medium containing 5 mM guanidine hydrochloride (Tuite et al., 1981). A *MATa [psi$^-$] [PIN$^+$]* but otherwise isogenic strain (YJW 564) was obtained by transient overexpression of Hsp104p in a sister spore of YJW 508. The *[PSI$^+$] [pin$^-$]* derivative (YJW 616) was obtained as described in Figure 1A. Unless otherwise noted, all yeast methods were as described in (Sherman, 1991). Deletions of *HSP104*, *NEW1*, and *RNQ1* were made using heterologous gene replacement (Longtine et al., 1998). *SUP35* was disrupted by omega integration of a linear DNA fragment consisting of the *TRP1* open reading frame flanked by the 500 base pairs on either side of *SUP35*.

Plasmid Construction

High-copy yeast plasmids were derived from pRS424, pRS425, and pRS426, while low-copy plasmids were derived from pRS314 and pRS315 (Christianson et al., 1992). All yeast expression vectors used a previously described modular system (Santoso et al., 2000) composed of a promoter flanked by 5′ XhoI and 3′ BamHI/SalI sites, a Gln/Asn-rich domain module flanked by 5′ BamHI/SalI and 3′ BglII/EcoRI sites, and in-frame GFP/CFP/YFP/EF modules flanked by 5′ BglII/EcoRI and 3′ SacI/NotI sites.

Sup35p$_{CA}$-GFP, New-GFP, and New-EF constructs were described previously (Santoso et al., 2000); for two-color fluorescence experiments, the GFP modules of these constructs were replaced by the appropriate GFP variant (Clontech). Other Gln/Asn-rich domains were amplified by PCR from yeast genomic DNA using oligonucleotides with 5′ BamHI or SalI and 3′ EcoRI linkers and cloned into the above vectors.

Construction of polyGln-expanded MJD fragment: to avoid genetic instability associated with pure CAG repeats, we designed complementary oligonucleotides encoding multiples of 20 glutamine residues using a mixture of CAG and CAA codons. These were annealed and inserted into the KpnI and BamHI sites of a bacterial shuttle vector. Inserting additional such cassettes into the resulting construct increased the polyGln tract in increments of 20. The polyGln tracts were inserted after residue 14 of a truncated MJD fragment (residues 203–284) (Ikeda et al., 1996), which was then introduced into the GFP expression system described above.

High copy expression plasmids bearing *HSP104*, *SSA1*, and *SSB1* were constructed by amplification from genomic DNA of these ORFS, as well as 500 bp on either side, followed by cloning into pRS423.

Truncation constructs of New1p were generated by amplification of the DNA sequences corresponding to the indicated codons flanked by 5′ BamHI and 3′ EcoRI sites followed by cloning into the modular GFP vectors described above. For constructs missing the natural initiator codon, ATG was introduced prior to the first indicated codon. The EE tag (Feschenko et al., 1992) was introduced by annealing two complementary oligonucleotides flanked by EcoRI and SacI sites and inserting them in place of GFP. New-GFP RR point mutants were generated using the QuickChange method (Stratagene).

Prion Induction Assays

Gene expression from high-copy plasmids was induced with 50 μM $CuSO_4$ for ~48 hr. Serial dilutions were plated onto synthetic medium lacking adenine (−ade) and rich synthetic medium. In all cases except in the Δ*new1* strain (as noted in Table 1), ADE+ colonies were counted after 5 days of growth. To generate *[NU$^+$]* strains, we replaced the plasmid-borne *SUP35* gene in *[pin$^-$]* and *[PIN$^+$]* derivates of a Δ*sup35* strain with a low copy plasmid expressing New-EF from the *SUP35* promoter, then transiently overexpressed New-GFP and selected for ADE+ colonies as above.

Cytoduction

A *[nu$^-$] [PIN$^+$] [rho$^-$] mata kar1-Δ13 sup35::TRP1 cyh2* pRS315-NEW-EF recipient strain was grown to log phase, mixed equally with similar cultures of *[nu$^-$]* or *[NU$^+$] [PIN$^+$] [RHO$^+$] mat*α *KAR1 sup35::TRP1 CYH2* pRS315-NEW-EF donor strains, and spotted onto YEPD plates. After 8 hr, the spots were streaked or patched onto YEPGlycerol with 10 μg/ml cyclohexemide, on which only *[RHO$^+$] cyh2* cytoductants can grow (Rose and Fink, 1987). Patches and individual colonies from each cross were tested for ADE+.

Fluorescent Microscopy and In Vivo GFP Foci Formation Assays

Yeast treated as in the prion induction assays above were examined by fluorescent microscopy (Zeiss Axiovert S100) through appropriate filters (Chroma) and photographed by CCD camera (Diagnostic Instruments Model 1.3.0). In aggregate counting experiments, at least five random fields with approximately 25–80 cells were examined by bright field microscopy, then by fluorescent microscopy; ratios reported indicate fraction of total cells displaying foci. Each experiment was performed at least 3 times; reported values are cumulative.

Other Assays

Centrifugation was performed as described previously (Patino et al., 1996; DePace et al., 1998), using ~100 μl final lysate volumes. MJD-GFP centrifugation was performed with the addition of 1% Triton X-100 to the lysis buffer. Fractions were resuspended in SDS-PAGE loading buffer with 4 M urea. For immunoblotting, polyclonal rabbit α-Sup35p (Santoso et al., 2000) and monoclonal α-GFP (Roche) sera were used.

Acknowledgments

We thank I. Derkatch, M. Bradley, and S. Liebman for sharing data prior to publication. We thank O. Weiner, M. Heiman, A. Santoso, M. Diamond, and members of the Weissman and Lim labs for helpful discussion. This work was supported by the Searle Scholars Program, the David and Lucile Packard Foundation, the NIH, and the HHMI. L.Z.O. is an HHMI Predoctoral Fellow.

Received April 20, 2001; revised June 29, 2001.

References

Bence, N.F., Sampat, R.M., and Kopito, R.R. (2001). Impairment of the ubiquitin-proteasome system by protein aggregation. Science *292*, 1552–1555.

Carmichael, J., Chatellier, J., Woolfson, A., Milstein, C., Fersht, A.R., and Rubinsztein, D.C. (2000). Bacterial and yeast chaperones reduce both aggregate formation and cell death in mammalian cell models of Huntington's disease. Proc. Natl. Acad. Sci. USA *97*, 9701–9705.

Chernoff, Y.O., Lindquist, S.L., Ono, B., Inge-Vechtomov, S.G., and Liebman, S.W. (1995). Role of the chaperone protein Hsp104 in propagation of the yeast prion-like factor. Science *268*, 880–884.

Chernoff, Y.O., Newnam, G.P., Kumar, J., Allen, K., and Zink, A.D. (1999). Evidence for a protein mutator in yeast: role of the Hsp70-related chaperone ssb in formation, stability, and toxicity of the [PSI] prion. Mol. Cell. Biol. *19*, 8103–8112.

Christianson, T.W., Sikorski, R.S., Dante, M., Shero, J.H., and Hieter, P. (1992). Multifunctional yeast high-copy-number shuttle vectors. Gene *110*, 119–122.

DePace, A.H., Santoso, A., Hillner, P., and Weissman, J.S. (1998). A critical role for amino-terminal glutamine/asparagine repeats in the formation and propagation of a yeast prion. Cell *93*, 1241–1252.

Derkatch, I.L., Chernoff, Y.O., Kushnirov, V.V., Inge-Vechtomov, S.G., and Liebman, S.W. (1996). Genesis and variability of [PSI] prion factors in Saccharomyces cerevisiae. Genetics *144*, 1375–1386.

Derkatch, I.L., Bradley, M.E., Zhou, P., Chernoff, Y.O., and Liebman, S.W. (1997). Genetic and environmental factors affecting the de novo appearance of the [PSI+] prion in Saccharomyces cerevisiae. Genetics *147*, 507–519.

Derkatch, I.L., Bradley, M.E., Masse, S.V., Zadorsky, S.P., Polozkov, G.V., Inge-Vechtomov, S.G., and Liebman, S.W. (2000). Dependence and independence of [PSI+] and [PIN+]: a two-prion system in yeast? EMBO J. *19*, 1942–1952.

Derkatch, I.L., Bradley, M.E., Hong, J.Y., and Liebman, S.W. (2001). Prions affect the appearance of other prions: the story of *[PIN$^+$]*. Cell *106*, this issue, 171–182.

Eaglestone, S.S., Cox, B.S., and Tuite, M.F. (1999). Translation termination efficiency can be regulated in Saccharomyces cerevisiae by environmental stress through a prion-mediated mechanism. EMBO J. *18*, 1974–1981.

Feschenko, M.S., Zvaritch, E.I., Hofmann, F., Shakhparonov, M.I., Modyanov, N.N., Vorherr, T., and Carafoli, E. (1992). A monoclonal antibody recognizes an epitope in the first extracellular loop of the plasma membrane Ca^{2+} pump. J. Biol. Chem. *267*, 4097–4101.

Ikeda, H., Yamaguchi, M., Sugai, S., Aze, Y., Narumiya, S., and Kakizuka, A. (1996). Expanded polyglutamine in the Machado-Joseph disease protein induces cell death in vitro and in vivo. Nat. Genet. *13*, 196–202.

Jung, G., and Masison, D.C. (2001). Guanidine hydrochloride inhibits Hsp104 activity in vivo: a possible explanation for its effect in curing yeast prions. Curr. Micro. *43*, 7–10.

Kopito, R.R. (2000). Aggresomes, inclusion bodies, and protein aggregation. Trends Cell Biol. *12*, 524–530.

Krobitsch, S., and Lindquist, S. (2000). Aggregation of huntingtin in yeast varies with the length of the polyglutamine expansion and the expression of chaperone proteins. Proc. Natl. Acad. Sci. USA *97*, 1589–1594.

Kushnirov, V.V., and Ter-Avanesyan, M.D. (1998). Structure and replication of yeast prions. Cell *94*, 13–16.

Lindquist, S., Patino, M.M., Chernoff, Y.O., Kowal, A.S., Singer, M.A., Liebman, S.W., Lee, K.H., and Blake, T. (1995). The role of Hsp104 in stress tolerance and [PSI+] propagation in Saccharomyces cerevisiae. Cold Spring Harb. Symp. Quant. Biol. *60*, 451–460.

Liu, J.J., and Lindquist, S. (1999). Oligopeptide-repeat expansions modulate 'protein-only' inheritance in yeast. Nature *400*, 573–576.

Longtine, M.S., McKenzie, A., 3rd, Demarini, D.J., Shah, N.G., Wach, A., Brachat, A., Philippsen, P., and Pringle, J.R. (1998). Additional modules for versatile and economical PCR-based gene deletion and modification in Saccharomyces cerevisiae. Yeast *14*, 953–961.

Michelitsch, M.D., and Weissman, J.S. (2000). A census of glutamine/asparagine-rich regions: implications for their conserved function and the prediction of novel prions. Proc. Natl. Acad. Sci. USA *97*, 11910–11915.

Muchowski, P.J., Schaffar, G., Sittler, A., Wanker, E.E., Hayer-Hartl, M.K., and Hartl, F.U. (2000). Hsp70 and hsp40 chaperones can inhibit self-assembly of polyglutamine proteins into amyloid-like fibrils. Proc. Natl. Acad. Sci. USA *97*, 7841–7846.

Newnam, G.P., Wegrzyn, R.D., Lindquist, S.L., and Chernoff, Y.O.

(1999). Antagonistic interactions between yeast chaperones Hsp104 and Hsp70 in prion curing. Mol. Cell. Biol. *19*, 1325–1333.

Patino, M.M., Liu, J.J., Glover, J.R., and Lindquist, S. (1996). Support for the prion hypothesis for inheritance of a phenotypic trait in yeast. Science *273*, 622–626.

Paushkin, S.V., Kushnirov, V.V., Smirnov, V.N., and Ter-Avanesyan, M.D. (1996). Propagation of the yeast prion-like [psi+] determinant is mediated by oligomerization of the SUP35-encoded polypeptide chain release factor. EMBO J. *15*, 3127–3134.

Perutz, M.F. (1999). Glutamine repeats and neurodegenerative diseases: molecular aspects. Trends Biochem. Sci. *24*, 58–63.

Perutz, M.F., Johnson, T., Suzuki, M., and Finch, J.T. (1994). Glutamine repeats as polar zippers: their possible role in inherited neurodegenerative diseases. Proc. Natl. Acad. Sci. USA *91*, 5355–5358.

Prusiner, S.B. (1998). Prions. Proc. Natl. Acad. Sci. USA *95*, 13363–13383.

Rose, M.D., and Fink, G.R. (1987). KAR1, a gene required for function of both intranuclear and extranuclear microtubules in yeast. Cell *48*, 1047–1060.

Santoso, A., Chien, P., Osherovich, L.Z., and Weissman, J.S. (2000). Molecular basis of a yeast prion species barrier. Cell *100*, 277–288.

Satyal, S.H., Schmidt, E., Kitagawa, K., Sondheimer, N., Lindquist, S., Kramer, J.M., and Morimoto, R.I. (2000). Polyglutamine aggregates alter protein folding homeostasis in Caenorhabditis elegans. Proc. Natl. Acad. Sci. USA *97*, 5750–5755.

Scherzinger, E., Sittler, A., Schweiger, K., Heiser, V., Lurz, R., Hasenbank, R., Bates, G.P., Lehrach, H., and Wanker, E.E. (1999). Self-assembly of polyglutamine-containing huntingtin fragments into amyloid-like fibrils: implications for Huntington's disease pathology. Proc. Natl. Acad. Sci. USA *96*, 4604–4609.

Serio, T.R., and Lindquist, S.L. (1999). [PSI+]: an epigenetic modulator of translation termination efficiency. Annu. Rev. Cell Dev. Biol. *15*, 661–703.

Sherman, F. (1991). Getting started with yeast. Methods Enzymol. *194*, 3–21.

Sondheimer, N., and Lindquist, S. (2000). Rnq1: an epigenetic modifier of protein function in yeast. Mol. Cell *5*, 163–172.

Sondheimer, N., Lopez, N., Craig, E.A., and Lindquist, S. (2001). The role of Sis1 in the maintenance of the [RNQ+] prion. EMBOJ *20*, 2435–2442.

True, H.L., and Lindquist, S.L. (2000). A yeast prion provides a mechanism for genetic variation and phenotypic diversity. Nature *407*, 477–483.

Tuite, M.F., Mundy, C.R., and Cox, B.S. (1981). Agents that cause a high frequency of genetic change from [psi+] to [psi-] in Saccharomyces cerevisiae. Genetics *98*, 691–711.

Warrick, J.M., Chan, H.Y., Gray-Board, G.L., Chai, Y., Paulson, H.L., and Bonini, N.M. (1999). Suppression of polyglutamine-mediated neurodegeneration in Drosophila by the molecular chaperone HSP70. Nat. Genet. *23*, 425–428.

Wickner, R.B., Taylor, K.L., Edskes, H.K., Maddelein, M.L., Moriyama, H., and Roberts, B.T. (1999). Prions in Saccharomyces and Podospora spp.: protein-based inheritance. Microbiol. Mol. Biol. Rev. *63*, 844–861.

Wickner, R.B., Taylor, K.L., Edskes, H.K., and Maddelein, M.L. (2000). Prions: portable prion domains. Curr. Biol. *10*, R335–R337.

Zhou, P., Derkatch, I.L., and Liebman, S.W. (2001). The relationship between visible intracellular aggregates that appear after overexpression of Sup35 and the yeast prion-like elements [PSI+]. Mol. Microbiol. *39*, 37–46.